Institute of Paper Science and Technology
Atlanta, Georgia

IPST TECHNICAL PAPER SERIES

NUMBER 470

RELATIVE FLOW POROSITY IN PAPER

J.D. LINDSAY

MARCH 1993

Relative Flow Porosity in Paper

J.D. Lindsay

Submitted to
Oxford Fundamental Research Symposium
September 1993
Oxford, England

Table of Contents

RELATIVE FLOW POROSITY IN PAPER

Jeffrey D. Lindsay
Associate Professor
Institute of Paper Science and Technology
Atlanta, GA 30318

ABSTRACT

Relative flow porosity is defined as the fraction of the void volume in a porous medium through which fluid can flow under a macroscopic pressure gradient. In saturated paper, much of the void volume is occupied by water that cannot flow due to chemical or physical absorption and mechanical obstruction (isolated or dead-end pores). In partially saturated paper, surface tension effects further hinder fluid flow through the sheet. In this paper, we discuss various methods for examining relative flow porosity and present results of new experimental techniques based on in-plane flow measurements. The experimental approach involves radially injecting known volumes of aqueous, non-absorbing dye into the center of a compressed, saturated sheet restrained by solid surfaces. The volume of the sheet occupied by the dye is measured, as is the total porosity of the sheet. The ratio of injected dye volume to pore volume within the dyed region is an estimate of effective porosity.

We show that in unrefined, filler-free paper, effective porosity values are on the order of 40% or more. The relative porosity may be as high as 90% of the extrafiber pore volume. Data for both initially dry and initially saturated sheets are presented. A geometric theory exists to predict relative porosity in fibrous structures, but we find that this model predicts

values for relative porosity much lower than we observe here. Using simple measures of the volume occupied by the swollen fibers in a compressed mat, we find that most (on the order of 90%) of the extrafiber pore space is available to flow.

INTRODUCTION

When water or other fluids flow in paper, much of the pore space is inaccessible to the flow. By definition, the pore space includes everything that is not cellulose or other solids, and thus includes water that is chemically bound or physically immobilized. In addition to water trapped in the cell wall or in the lumen, the arrangement of fibers in the sheet can create large dead-end pores or stagnant regions which are unlikely to participate in flow. Pressing the paper can compress these zones and drive fluid out, but in the presence of a hydraulic pressure gradient alone, flow is unlikely to occur in these regions.

To better characterize and understand fluid flow in fibrous structures such as paper, it will be useful to know what fraction of the pore space is available for fluid flow. This issue is particularly relevant to problems of infiltration or penetration, as in sizing, coating, and printing. In the case of penetration by an immiscible phase, two-phase partitioning and relative permeability effects also become important. An example is displacement dewatering, in which a gas is used to displace liquid water from a web. The amount of water removal possible will be affected by the amount of water in pores open to flow.

We define the fraction of the void volume that is available to fluid flow as the relative flow porosity, ε_{rel}, which has possible values between 0 and 1. (For convenience, we will refer to the relative flow porosity as simply the relative porosity.) Note that the effective flow porosity, ε_{eff}, defined as the fraction of the total paper volume open to flow, is the product of relative porosity and total porosity, ε, with total porosity defined as the volume fraction of pore space. In addition, we need to distinguish the pores between fibers from the micropores contained in the swollen cell

wall. If we treat the swollen fiber as a solid structure, the volume fraction of the remaining pore space is the extrafiber porosity, ε_o. These concepts are summarized in Table 1.

Term	Definition
Total porosity, ε	Volume fraction of pore space, or 1 - volume fraction of solid matrix
Effective flow porosity, ε_{eff}	Volume fraction of pore space open to flow
Relative flow porosity, ε_{rel}	Fraction of the total pore space that is open to flow: $\varepsilon_{rel} = \varepsilon_{eff}/\varepsilon$
Extrafiber porosity, ε_o	Volume fraction of pore space between swollen fibers, or 1 - volume fraction of swollen fibers

Table 1. Porosity Definitions.

This paper aims to present data on effective porosity for paper, and to compare it with other means of characterizing fiber-fluid interactions in fibrous structures.

Relative porosity is especially important when two phases are involved, as when gas displaces liquid, for it governs the speed of the phase boundary. In other words, the penetrating phase can only move through the open, interconnected pores. If the effective porosity of this pore space is small, the penetrating fluid boundary may advance rapidly, yet the amount of penetrating fluid will be small. In two-phase flows, however, capillary effects can cause one phase to obstruct the flow of the other phase, further reducing the effective flow porosity open to each phase.

ESTIMATES OF RELATIVE POROSITY USING PRIOR DATA AND THEORY

In this section, we will find that a variety of concepts in the literature are useful in understanding the distribution of water in a sheet, and can be used to make estimates of relative porosity if we assume that all the pore space outside the swollen cell wall of paper is available to flow. Such logic, however, would imply $\varepsilon_{rel} = 1$ in an unswollen fibrous structure.

A previous study will then be discussed in which a theoretical estimate for relative porosity in an unswollen fibrous web is made. We will modify this result for swollen fibers to obtain a basis for comparing our experimental results reported below.

Extrafiber Pore Space

For paper, the relation between pore space and effective porosity is complicated by the swollen nature of the solid matrix. As a first approximation, one could assume that all the pore space between the swollen fibers in wet paper is available to flow. In other words, ε_o, the extrafiber pore space, might approximate ε_{eff}. In reality, some of the extrafiber pore space will include dead-end pores and possibly other zones of stagnant fluid, so ε_{eff} may be less than ε_o. For now, however, we will neglect the difference.

Water retention ratios.

There are several ways to estimate ε_o. For a computer model of wet pressing, Roux and Vincent (1) estimate it using the water retention ratio (WRR, also called water retention value, WRV) of pulp, reported as grams of water per gram of dry fiber, a measure of the water still held by the fibers after centrifugal dewatering. Effective porosity can then be expressed as:

$$\varepsilon_{eff} \approx \varepsilon_o = \varepsilon - WRR \frac{\rho_s}{\rho_l} (1-\varepsilon), \qquad (1)$$

where ρ_s is the dry solid density, generally taken as 1.55 g/cm^3 for cellulose, and ρ_l is the liquid density, 1.0 g/cm^3 for water. Relative porosity is then

$$\varepsilon_{rel} = 1 - WRR\frac{\rho_s}{\rho_l}\left(\frac{1-\varepsilon}{\varepsilon}\right). \quad (2)$$

The difficulty here is that WRR depends on the somewhat arbitrary procedure used, and is not necessarily a valid description of fiber-water interactions in a compressed web. Using a "typical" WRR of 1.7 for a lightly refined chemical pulp, the relationship between total porosity and relative porosity is shown as one of two curves in Figure 1. Once the porosity of a sheet has been reduced below 0.725, Equation 2 yields negative, physically impossible relative porosities. In reality, water will be expressed from the cell wall and from trapped pores as the sheet is compressed, reducing the amount of water retained in the swollen fibers. The experimentally measured WRR is for an essentially uncompressed state. Use of WRR to estimate relative porosity in a paper web is therefore questionable.

Ellis (2) used unusually high g-forces (up to 5x10^4 g, compared to normally used values of 3000 g or less) in a series of WRR measurements to determine the limits on water removal by mechanical forces. Extrapolating his data for several pulps to even higher g-forces, he determined that a WRR value of 0.5 represented the expected maximum degree of water removal possible by mechanical forces. A WRR of 0.5 represents 33% moisture or 67% solids. A second curve is shown in Figure 2 for a WRR of 0.5. If a water-saturated sheet is compressed to the point where no interfiber pores exist and the WRR is 0.5, then the total porosity at this point is 43.7%, the point at which relative porosity goes to zero. In wet pressing of paper, practical porosity values of the wet sheet are expected to lie between 50 and 80%.

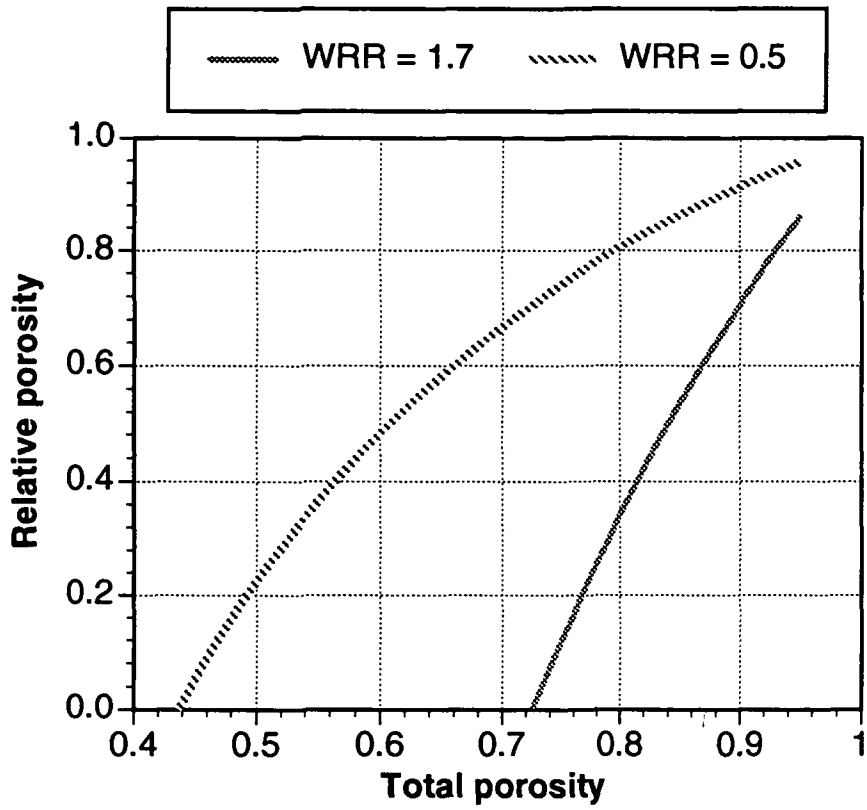

Figure 1. Estimated relative porosities from Equation 2 for two WRR values.

Other measures of associated water.

A variety of other techniques have been applied to determine the water retained in the cell wall. Robertson (3,4) compares water of association estimates using several techniques (hydrostatic tension, permeability, and dye migration) in uncompressed or lightly compressed webs. Most values were over 2 gm of water per gm of fiber and may not be useful in describing the pore state of a paper web beyond the forming section of a papermachine.

The solute exclusion technique of Stone and Scallan (5) has also been useful in identifying the amount of water contained in micropores (pores

inaccessible to dextran of a specified molecular weight) in the cell wall. Solute exclusion results are generally consistent with Ellis's high-g WRR results (micropore water content on the order of 30% or greater). Carlsson et al. (6) applied a related method to show that associated water is expressed from micropores as paper is pressed to higher solids levels. One may assume that the water in micropores is trapped and unavailable for flow under an external pressure gradient, but this is not necessarily the case. Some pores may permit throughflow. However, the velocity through such pores will be much smaller for a given pressure gradient than in larger interfiber pores, and their contribution to flow may be negligible.

Kozeny-Carman Analysis

Permeability measurements in paper can be applied to estimate the amount of water immobilized by the swollen fiber. Here permeability is defined as the empirical constant, K, in Darcy's law for unidirectional flow in porous media:

$$v = \frac{K}{\mu}\frac{\Delta P}{L}, \tag{3}$$

where v is the superficial velocity (flow rate divided by area), μ is the fluid viscosity, and ΔP is the pressure drop in the flow direction across a distance L. K, the permeability, has units of length squared.

The permeability of a deformable porous medium changes as it is compressed. Formulas relating permeability and porosity can be derived by making simplifying assumptions about the structure of the medium. For example, by assuming that the pore network consists of many distinct, continuous, and regular channels passing from one end of the porous medium to another, the well-known Kozeny-Carman equation can be obtained:

$$K = \frac{1}{\kappa S_o^2}\frac{\varepsilon_o^3}{(1-\varepsilon_o)^2} \tag{4}$$

where S_o is the surface area per unit volume of solid material, and κ is a shape factor (the Kozeny constant) that accounts for effects of channel shape and orientation. Note that we have used ε_o instead of ε (which is usually seen in the Kozeny-Carman equation), for the pore space considered in the derivation is the extrafiber pore space. The water trapped in the cell wall presumably does not contribute to flow and in effect increases the apparent volume of the solid (immobile) phase.

The Kozeny constant, κ, can be derived for ideal, simple pore structures, but becomes an empirical factor for real porous media. In many cases, it is not constant but a function of porosity. For fibrous media, a value of 5.55 is a widely used value which works well in many cases (7), although values typically may lie in the range of 3-7 for porosities less than 0.8 (8). When an empirical factor is used, the effect of dead-end pores and other regions of immobilized fluid on the average velocity or on the permeability is accounted for, but no information about the relative porosity itself can de derived. We will again assume that ε_o approximates ε_{eff}.

The effective volume of the swollen fibers is defined as α, with units of cm^3/g. At a concentration of c g/cm^3, the extrafiber porosity is

$$\varepsilon_o = 1 - \alpha c \tag{5}$$

which can be used instead of ε in Equation 4, with the assumption that κ = 5.55, to yield

$$K = \frac{1}{5.55 S_o^2} \frac{(1-\alpha c)^3}{\alpha^2 c^2}. \tag{6}$$

Now we note that $\alpha S_o = S$, where S is the flow-exposed surface area of the fibers per unit mass, commonly called the specific surface area. Incorporating this definition into Equation 6 and rearranging, we obtain

$$(Kc^2)^{1/3} = \left(\frac{1}{5.55\ S^2}\right)^{1/3} (1-\alpha c) \tag{7}$$

which is a classic equation that has been applied frequently to pulp mats (9). By plotting permeability data from a single sample at various

compressive plots as $(Kc^2)^{1/3}$ versus c, the specific volume, α, can be obtained from the slope and the specific surface, S, can be obtained from the intercept.

We now present specific calculations from some of our measurements at IPST. Figure 2 shows permeability-versus-porosity data obtained in a study of linerboard pulp.

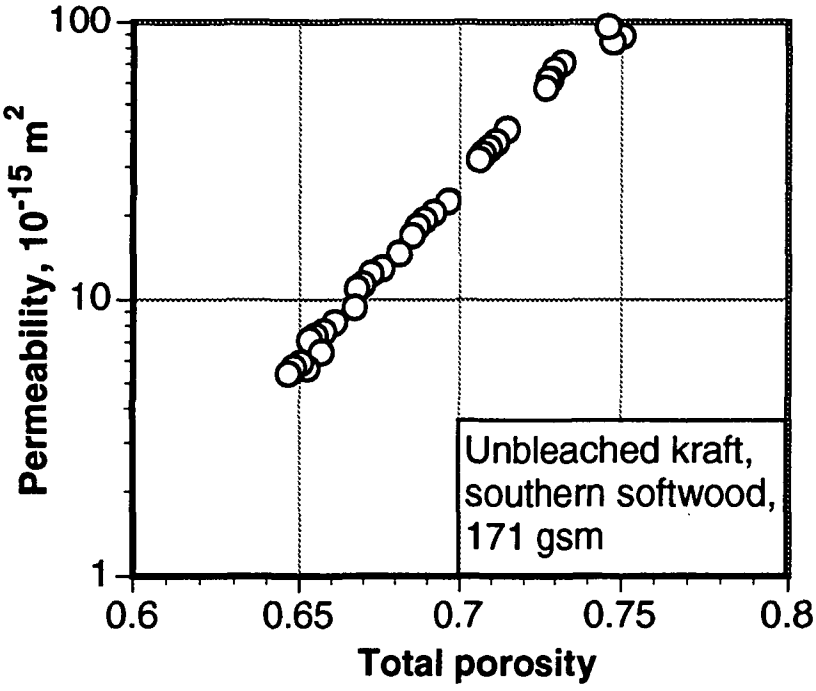

Figure 2. Permeability data for a handsheet of unbleached kraft pulp.

The same permeability data can then be reduced to obtain the following graph of $(Kc^2)^{1/3}$ versus c:

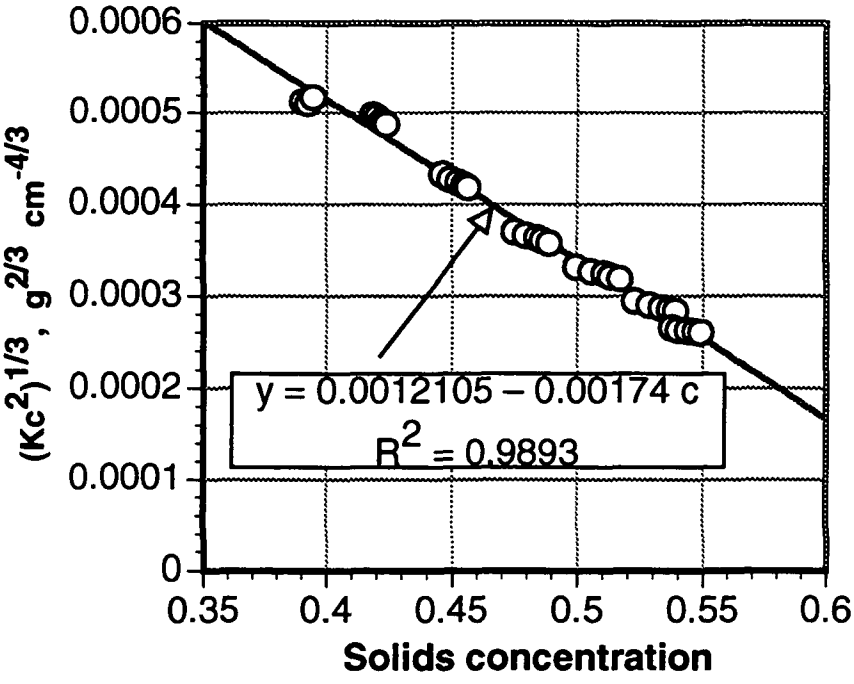

Figure 3. Permeability data from Figure 2 replotted for Kozeny-Carman analysis.

The slope and intercept results can be used to solve for S and α, in this case giving S = 1.01 m^2/g and α = 1.44 cm^3/g. If we assume $\varepsilon_{rel} = \varepsilon_o$, then α can be used with Equation 5 above to give

$$\varepsilon_{rel} \approx \frac{\varepsilon_o}{\varepsilon} = \frac{1-\alpha c}{\varepsilon} = \frac{1-\alpha\rho_s(1-\varepsilon)}{\varepsilon}. \qquad (8)$$

Figure 4 below shows ε_{rel} as a function of ε for several typical values of specific volume (based on IPST measurements for many pulp types), including the value of 1.44 cm^3/g from the example above. As with WRR, α will decrease with compression.

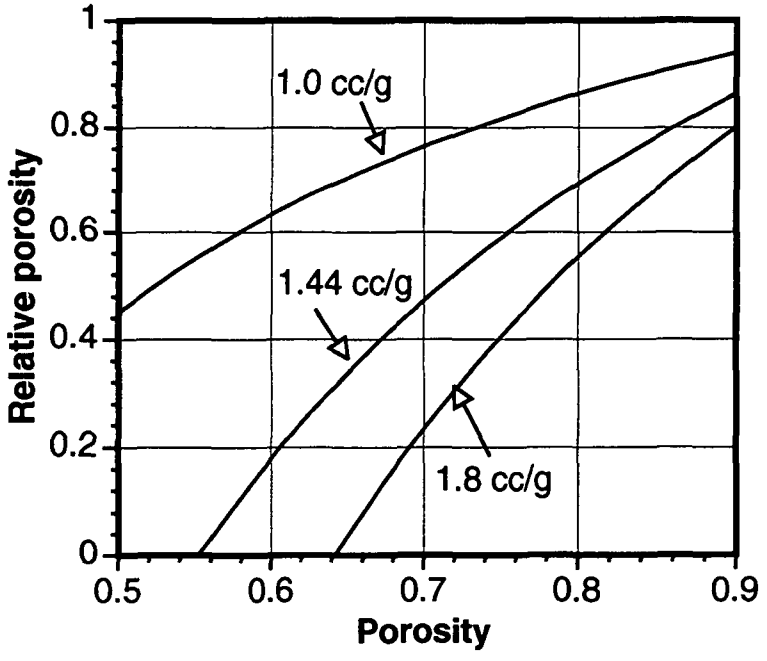

Figure 4. Relative porosity in paper based on Kozeny-Carman analysis using typical specific volume results.

Kyan's Geometrical Model

The topic of relative or effective flow porosity in fibrous media has not received extensive treatment in the past. Kyan et al. (10) treated the issue theoretically, deriving expressions for relative porosity based on geometrical considerations for a structure composed of cylindrical fibers arrayed in a regular pattern. They noted that the pressure drop for flow in fibrous structures tends to be surprisingly high given the typically high porosity of the webs. They postulated that one reason for the high pressure drop is that much of the pore space is occupied by stagnant fluid, or in other words, that the relative porosity is low. The derived expression for effective flow porosity is

$$\varepsilon_{eff} = N_e^2(1-\varepsilon)\,(0.5/\pi) \qquad (9)$$

where N_e is the effective porosity number,

$$N_e = \left(\frac{\pi}{0.5(1-\varepsilon)}\right)^{1/2} - 2.5. \qquad (10)$$

These formulae give relative porosity values, $\varepsilon_{eff}/\varepsilon$, much less than unity. For example, a fibrous web with a porosity of 50% would have ε_{rel} = 0.174. Figure 5 shows predicted relative porosity as a function of total porosity.

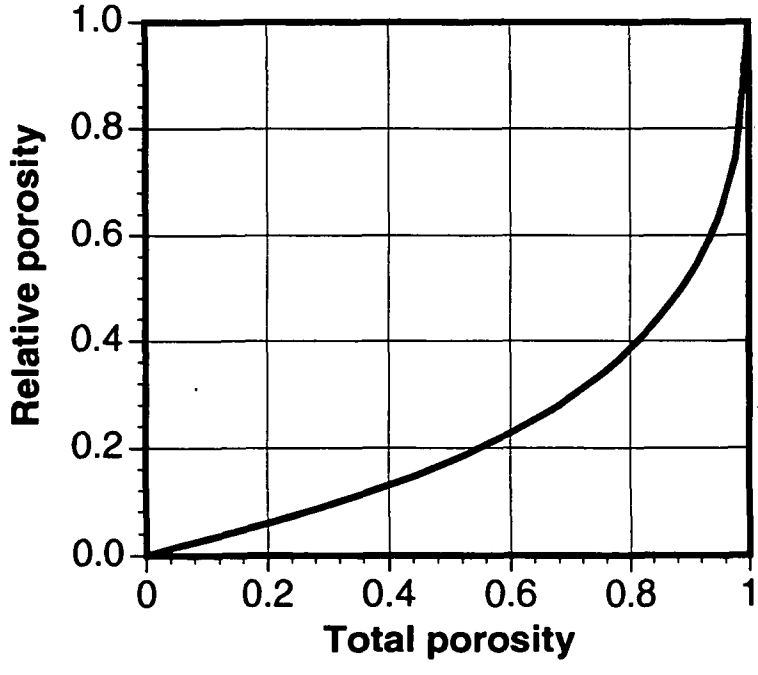

Figure 5. Predicted relative porosity based on the approach of Kyan et al. (10).

In the case of a swollen fiber, the porosity used in Equations 9 and 10 should be the extrafiber porosity, ε_o, if we assume that water trapped in the fiber does not flow. Again, we can use WRR or specific volume data to estimate ε_o as a function of ε, and then obtain new estimates for relative porosity based on Kyan's approach. The results are shown in Figure 6 for several values of specific volume, including the specific volume for completely unhydrated cellulose, 0.65 cc/g.

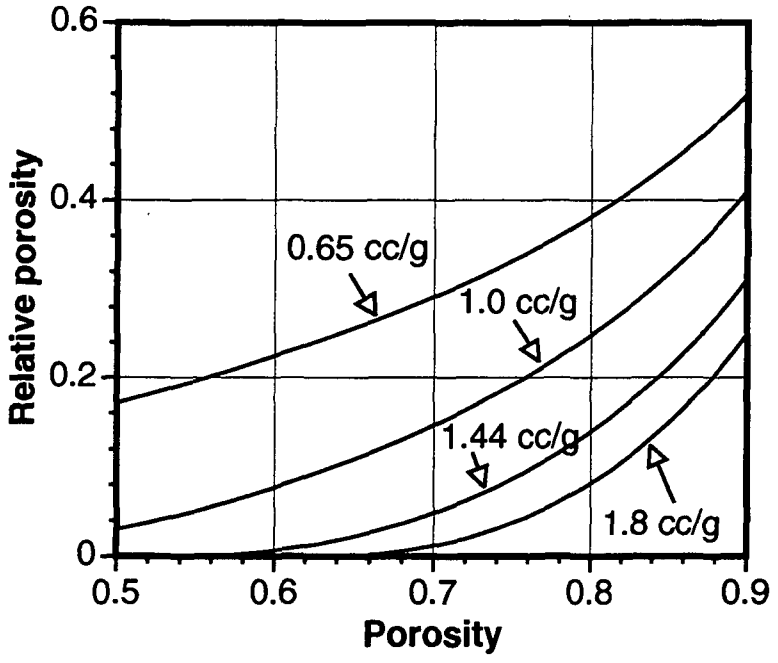

Figure 6. Relative porosity results based on a combination of Kyan's model (10) and extrafiber porosity analysis using typical specific volume values. Unhydrated fiber corresponds to α = 0.65 cc/g.

Significant reductions in relative porosity are predicted with swelling. In general, in the total porosity range of 0.6 to 0.75, where we expect typical furnishes to have specific volumes of roughly 1.0 cc/g or higher, the predicted relative porosity should be no more than 20%, based on our application of the only known model for relative porosity in a fibrous medium. In that same total porosity range, however, relative porosities as high as 80% could be achieved if the extra fiber pore space were free of dead-end pores and other zones of stagnant fluid. We will now test the applicability of the above analyses with experimental methods.

EXPERIMENTAL APPROACH

To estimate the relative porosity in fibrous structures, we extend experimental methods for in-plane fluid flow measurements that were developed at the Institute of Paper Science and Technology (11-14) and

at TRI (15-18). The concept we employ is in-plane radial injection of a colored fluid into the center of a disk of paper. The paper is restrained between two smooth, uniformly pressed platens, which seal the surfaces of the sheet and allow flow to occur only in the radial direction. As the dye spreads into the sheet, it flows through pores open to flow. By comparing the volume occupied by the injected dye in the sheet with the volume of dye actually injected, we can determine the relative porosity (details of the calculation are given below). This can be done for both saturated sheets and initially dry sheets, although dry sheets pose the risk of air bubbles hindering fluid penetration and decreasing the measured relative porosity.

For this study, we modified the IPST lateral permeability apparatus, which has been previously described (19). In order to observe the growth of a dyed region during in-plane fluid injection, we replaced a metal platen in the permeability apparatus with a device to allow optical access to the compressed sheet. The platen replacement is a large cube of clear, rigid plastic which will transmit force from the Carver press assembly to the paper, as shown in Figure 7. A metallic mirror oriented at 45° from horizontal was cast into a plastic cube, as shown in Figure 8. The use of a mirror to observe in-plane fluid flow was inspired by the work of Adams et al. (15-17) at TRI. The mirror allows a viewer or a camera standing in front of the cube to observe the paper while it is under compression between the plastic cube and the lower platen. The growth of a dyed zone, formed by injection of colored water through the lower platen, can be viewed during a run. Normally, only the final boundary of the dyed region is noted after a given volume of fluid has been injected.

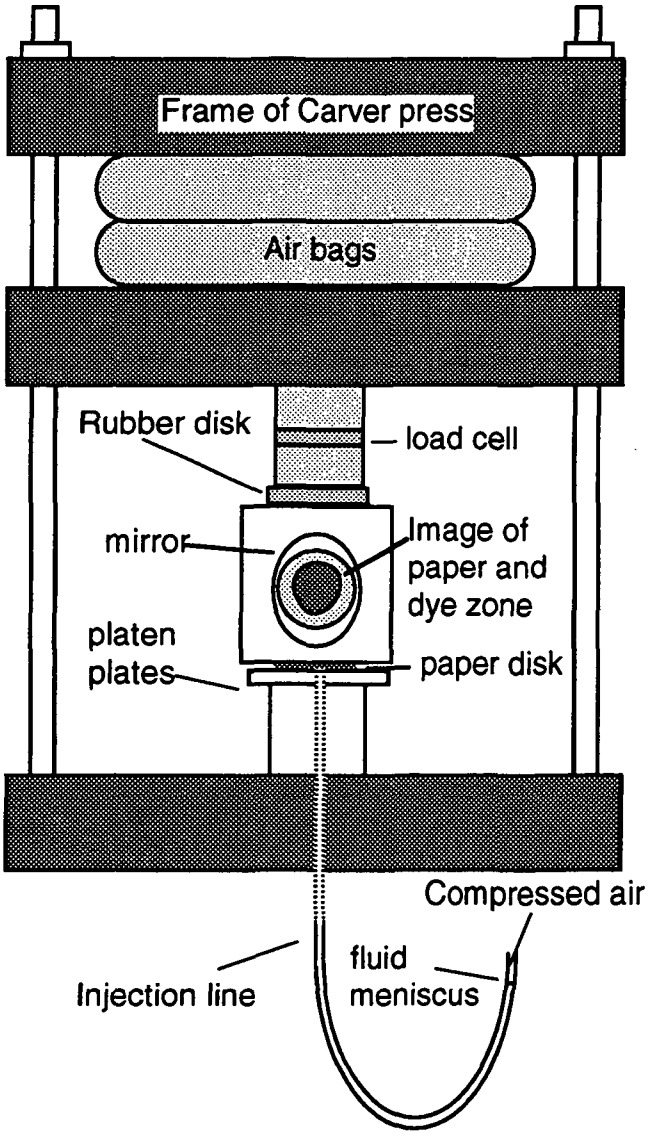

Figure 7. Modified lateral flow apparatus for dye injection tests.

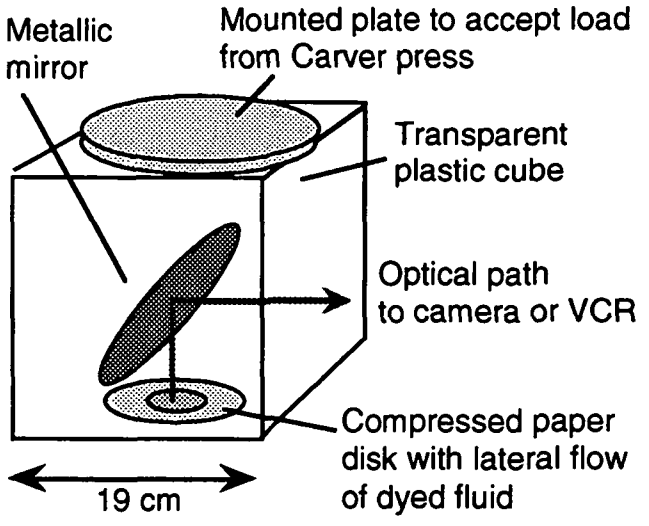

Figure 8. Plastic pressing block with mirror for optical access to a compressed sheet.

The idea of our method is simple: inject fluid into paper, and compare the volume of fluid injected to the volume of the dyed region (based on thickness and dyed area) multiplied by sheet porosity. Sheet porosity is determined from sheet thickness under compression and basis weight:

$$\varepsilon = 1 - \frac{BW}{\rho_c L}, \tag{10}$$

where BW is the sheet basis weight, ρ_c is the matrix density (e.g., the density of pure cellulose in filler-free sheets), and L is the sheet thickness. The area of the dyed zone can be measured after injection, or, if the sheet has been marked with measured lines, the dyed area can be determined at various intervals during dye injection by viewing the dye boundary through the plastic cube.

Thickness is determined from three LVDT sensors distributed around the lower platen. LVDT rods protrude from the lower surface of the plastic block. The signal from the sensors responds monotonically to the position of the rods in the sensor. The thickness readings from the three sensors are averaged to give the sheet thickness.

In sheets that were initially dry, saturation was performed under vacuum to reduce the presence of air bubbles in the sheet. We placed a dry sample on a support stand in a desiccator jar containing a layer of water at the bottom. The lid was placed on the jar and vacuum applied to deaerate the sheet. The jar was then bumped to knock the sample off its support, causing the sheet to fall into the water. After water infiltrated the pores of the sample, the vacuum was released.

The dye used in most of this study is Versatint Purple II (Milliken Chemical, Inman, S.C.), a fugitive water-soluble dye that does not absorb significantly onto cellulose. It was selected for its nonreactivity with paper fibers. We also conducted a number of tests using blue dextran 2000 (Pharmacia Fine Chemicals, Uppsala, Sweden), a strongly colored water-soluble polysaccharide that does not absorb onto paper. The high-molecular weight (ca. 2×10^6), highly-branched polymer is too large to pass through micropores in the paper, but can flow through interfiber pores.

Figure 9 is a photograph of a sample after dye injection has occurred. Some diffusion of dye occurred over a space of hours after the run was conducted. Lines were drawn to mark the original dye boundaries immediately after injection. The sample shown in Figure 9 was a machine-made paper. The dyed region is elliptical since the machine-direction permeability is slightly greater than the cross-direction permeability (11,14).

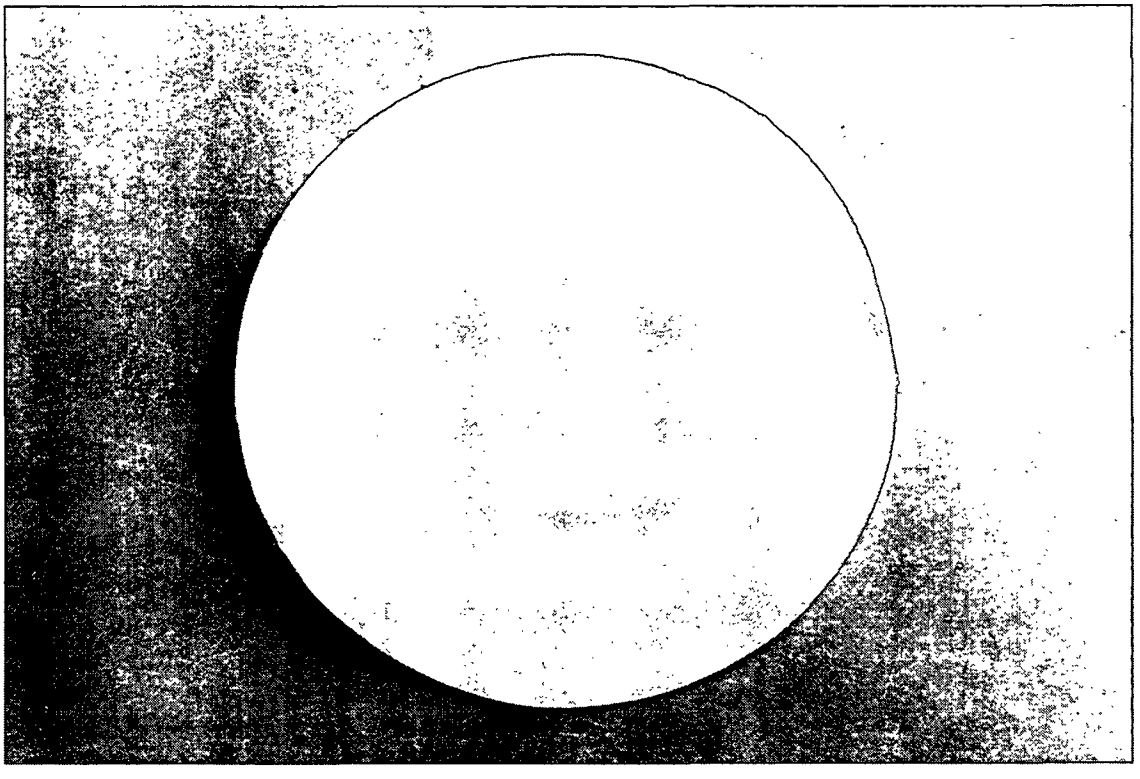

Figure 9. Blotter paper sample photographed after in-plane dye injection.

Problems to Consider

We assume that the dyed fluid directly displaces clear water in the pores open to flow. Diffusion will affect the results in several ways. First, diffusion will mix some of the dye with water in dead-end pores or micropores. This process will dilute the dye, but should have little effect on the observed motion of the dye boundary. Diffusion in the flow direction (radially outward) will inflate the apparent growth of the dyed region (thus deflating our estimate of effective porosity), but this effect is reduced in our tests by maintaining injection rates high enough such that the forced advance of the dye boundary is much greater than the motion due to diffusion. Likewise, when we inject dye into dry paper, we force boundary growth to be much faster than the growth due to capillary effects or diffusion.

In addition to diffusion, convective mixing in pores open to flow must be considered. Mixing in the flow direction is due to velocity gradients in the pore. For example, in laminar flow in a tube, a parabolic velocity profile exists. If a sharp boundary between dyed fluid and clear fluid exists initially, this boundary will soon be spread out in the flow direction as the fluid at the center of the tube moves more rapidly than the fluid at the walls. This effect is shown in Figure 10.

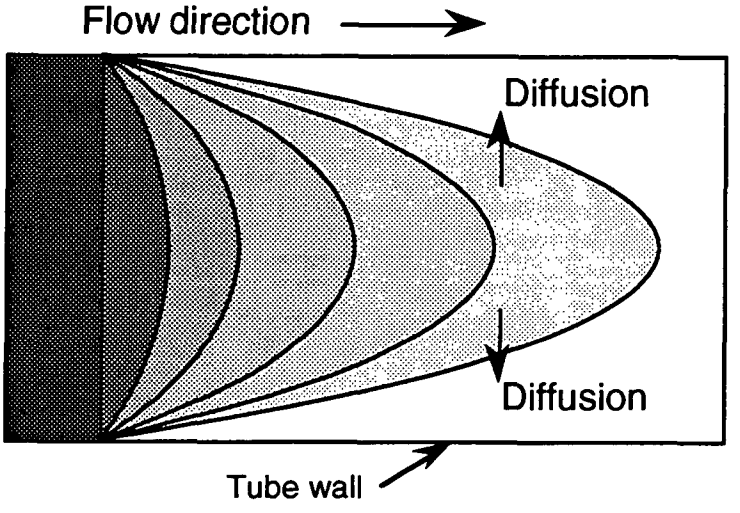

Figure 10. Distortion of a flat dye-water boundary moving in a flow with a parabolic velocity profile. Some of the dye advances faster than the average flow velocity.

If there were no diffusion, dye at the very center of the tube would flow at twice the average flow velocity, creating a broad gradient in concentration. In reality, dye from the fast-flowing center of the tube diffuses into the slow moving fluid near the wall. If the diffusion is rapid, the advancing dye front becomes sharp (assuming that the axial flow is fast compared to axial diffusion). This problem is known as Taylor dispersion and is treated by Cussler in (20).

Experimentally, the dye-water interface appears sharp, but Taylor dispersion in the flow direction certainly occurs to a degree. This will increase the apparent spread of the dye zone, and will deflate our

estimates of relative porosity. We will simply ignore dispersion and take our estimates as lower bounds for effective porosity.

As dye is injected into a 12.7-cm disk, the dye boundary can be measured at various locations. Since dispersion will increase with the distance traveled, we expect apparent relative porosity values to drop as the dye boundary progresses. Based on this concept, the dyed zone in the paper disk should be kept as small as possible. On the other hand, smaller dyed zones are more likely to be nonuniform from the top to the bottom of the sheet. The dyed region visible through the plastic block may be smaller than the dyed region in the middle or on the bottom of the sheet. For example, the surfaces of a handsheet may be slightly less porous than the interior, resulting in penetration of dye in the middle of the sheet that may not be immediately visible when viewed from above. The pressure distribution in the sheet near the injection port may also be nonuniform in the z-direction near the injection port. After a sufficient distance has been traveled, the dye becomes reasonable uniform from top to bottom. We have found that a diameter over 5 cm gives good results in terms of z-direction uniformity of the dyed boundary. If we determine relative porosity using smaller zones, two-sidedness in the dyed zone may inflate the estimate of relative porosity. In highly permeable samples, such as ceramic paper, good uniformity also requires higher injection rates.

As the boundary exceeds about 10 cm, a significant decrease in relative porosity may occur due to dispersion, depending on the pore structure. In making measurements, we generally inject enough dye to obtain a dye boundary between 5 and 10 cm. Below we will report observed changes in relative porosity with the size of the dyed zone.

RESULTS

In a variety of paper samples tested, we have found relative porosity to exceed 40% for compression below 700 kPa. We have obtained results for sheets made from virgin and recycled linerboard furnish, bleached softwood kraft handsheets, commercial blotter paper, and a specialty ceramic paper.

Wet Linerboard

While the dye injection method was designed for use with bleached paper, we also obtained useful results with an unbleached kraft furnish made from southern softwood (a commercial linerboard bottom sheet furnish). Relative porosity data were obtained for 200-gsm sheets. The pulp was never-dried. In one set of tests (Series A), we injected a quantity of dye into the sheets and then measured the size of dye zone after the sample was removed from the test apparatus. The dye zone diameters fell into the usual range of 6-10 cm. In Series B, we injected dye until it reached the boundary of the paper. We wished to track the dye motion in the sheet, but viewing the dark dye in the dark paper under compression was difficult. However, through the plastic cube we could easily see when dye began leaving the edge of the sheet. We varied load to obtain a small range of porosity values.

We also made measurements in a sheet made from the same furnish after recycling; i.e., handsheets made from the never-dried pulp were dried in a 105°C oven, then slurried and formed into a new 200-gsm handsheet. We compare the never-dried, virgin fiber handsheets with the recycled sheets in Figure 11. Also shown are results for a commercial OCC furnish from the same mill that produced the virgin linerboard furnish. The OCC and the recycled fibers have a higher relative porosity at a given true porosity than the never-dried pulp. Fibers that have been dried are expected to have a lower specific volume, resulting in relatively more interfiber pore space open to flow.

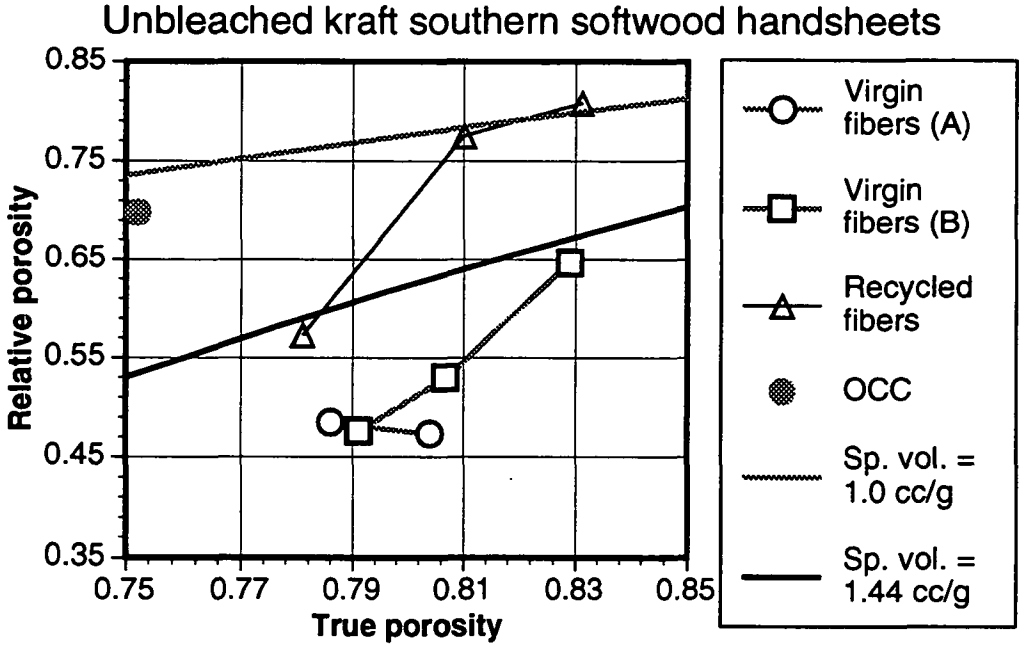

Figure 11. Relative porosity in virgin and recycled unbleached kraft sheets. Extrafiber pore space curves are also shown (see Figure 4).

We used the IPST permeability device (19) to measure the z-direction permeability to water of sheets made from virgin and recycled fibers. Measurements in five 200-gsm sheets of virgin fiber gave specific volume values between 1.39 and 1.55 cc/g. Measurements in three recycled sheets (made from dried and reslurried virgin fiber) gave specific volumes between 1.14 and 1.21 cc/g. The extrafiber porosity curves from Figure 4 for specific volumes of 1.0 cc/g and 1.44 cc/g are shown in Figure 11 for comparison. Specific volume data are difficult to obtain with accuracy for swollen fibers, and are based on a variety of empiricisms and inaccurate assumptions, making hydrodynamic specific volume only a rough estimate of the physical state of the compressed fibrous medium. However, if most or all of the extrafiber pore space is available to flow, we can say that our measurements of relative porosity in the virgin and recycled unbleached kraft sheets are roughly consistent with our estimates of extrafiber pore space derived from permeability measurements. Flow access to most of the extrafiber pore space strongly contradicts the geometrical model of Kyan et al. (10).

Bleached Papers

For a variety of bleached paper samples, we have consistently found relative porosity values above 40% for the total porosity range of 0.65 to 0.8. After vacuum deaeration and water infiltration, wet blotter paper disks were particularly easy to work with. In exploring relative porosity results in blotter paper (ca. 240 gsm), we were able to obtain enough data to examine the sensitivity of our results to the details of our procedures. In particular, we explored the effect that the size of the dye zone in the paper had on measured relative porosity. An effect is expected, as we discussed above, for dispersion and mixing will tend to decrease relative porosity as the dye boundary grows. However, we did not detect a significant dependence on dye zone diameter in the unbleached kraft sheets discussed above (e.g., similar results were obtained in virgin sheets for dye zones from 6 to 12.7 cm in diameter).

Relative porosity results for wet blotter paper as a function of dye zone diameter are shown in Figure 12. Results for four samples are shown, listed by the total porosity that existed during the measurement (all around 70% total porosity). Since blotter paper has directionality, with a machine direction permeability around 10-30% greater than the cross-direction permeability (11), the injected dye zone tends to be elliptical. When the dye zone was clearly elliptical as opposed to circular, the diameter we report is the average of the major and minor axes. In Figure 12, we see that the smallest diameters lead to the greatest effective porosity values. In these samples, we suspect that diameters of 5 cm and less are subject to errors due to z-direction nonuniformity of the dye, as discussed above. Our standard procedures call for taking measurements in the range of 7-10 cm, with higher diameters sometimes necessary. There is still considerable variability with diameter in this range, but we can bracket relative porosity within the range of 60-90% for these sheets. Using a specific volume of 1.0 cc/g for blotter paper, the available extrafiber porosity is around 75% for these sheets, which is in the middle of our range for relative porosity. It appears that very little of the extrafiber pore space is taken up by dead-end pores.

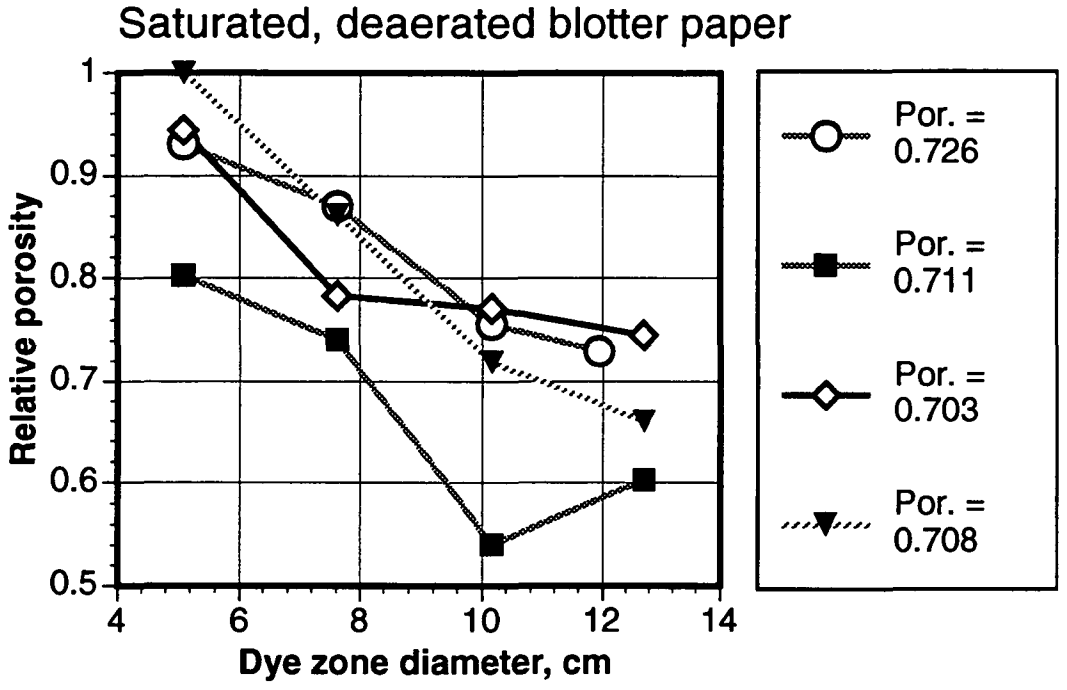

Figure 12. Relative porosity results in saturated blotter paper as a function of dye zone diameter injected into the sheet.

Some of our earliest measurements in this study were with handsheets from a bleached kraft southern softwood furnish. The furnish was relatively unrefined, with a freeness of 700 ml CSF. Results for several replicate tests are shown in Table 2. Good reproducibility was achieved. (The diameter of the dyed zone in these samples ranged from 4.7 to 5.6 cm.) At 81% total porosity, the geometric model of Kyan predicts that completely unhydrated fibers would have a relative porosity of 40%. Achieving a relative porosity of at least 45% (assuming our values are lower estimates) for a hydrated pulp (specific volume estimated at 1.2 g/cm^3) implies that the model of Kyan et al. (10) significantly under-predicts relative porosity for paper and possibly other fibrous materials.

Total porosity	Relative porosity
0.814	0.471
0.817	0.454
0.815	0.446
0.817	0.465
0.812	0.458
AVG:	**0.459**

Table 2. Replicate relative porosity values for tests with handsheets of never-dried bleached southern softwood kraft pulp.

Following three months of storage in a cold room, two additional handsheets of the bleached kraft softwood pulp were tested. Blue dextran 2000 was used as the dye. Similar results were obtained, as shown in Table 3.

Total porosity	Relative porosity
0.825	0.535
0.766	0.396

Table 3. Replicate relative porosity values for tests with handsheets of never-dried bleached southern softwood kraft pulp.

Subsequent tests were conducted in additional sheets to determine the effect of dye zone size on apparent relative porosity. Results for several sheets are shown in Figure 13. These sheets all had compressed total porosities in the range of 0.77 to 0.82. The effect of dye diameter appears strong for these samples. While dispersion can reduce the measured relative porosity as the dye diameter grows, an estimate of 40-50% is expected to be reasonable in this case. The true relative porosity could be higher. We have further work to do before we can overcome the problems of dispersion for large dye diameters (reducing the measured effective porosity) and poor visibility or dye nonuniformity for smaller diameters (inflating measured effective porosity). Numerical modeling may be needed to determine the optimum technique for measurement.

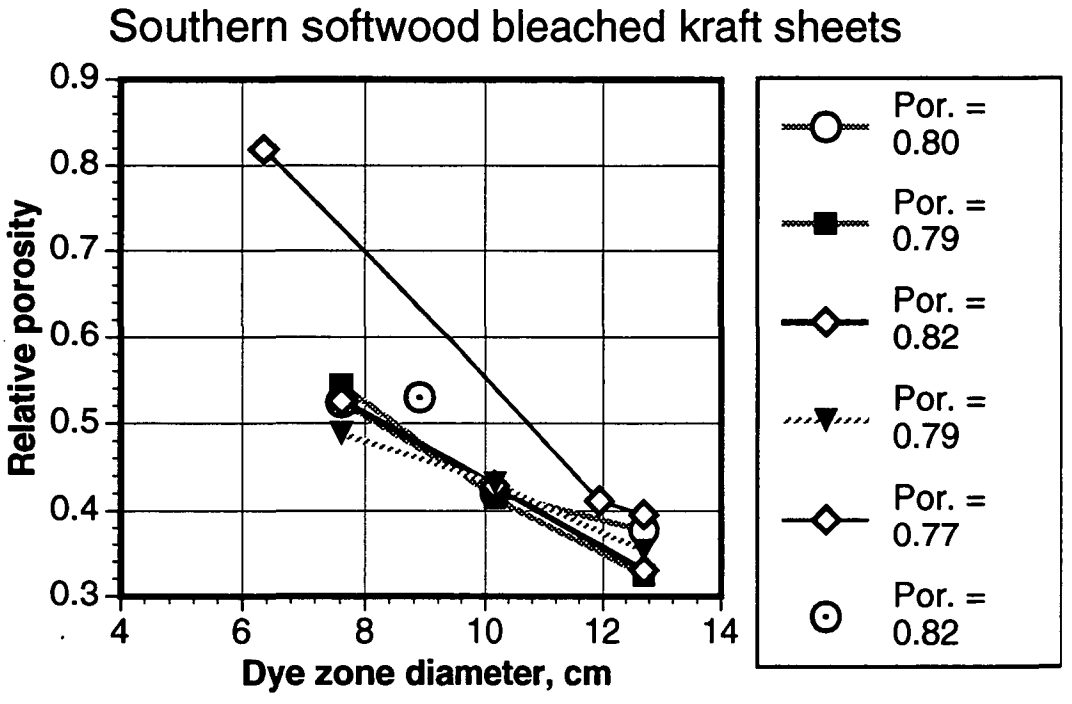

Figure 13. Relative porosity versus dye diameter in bleached kraft handsheets.

Ceramic Paper

We have also tested samples of ceramic paper produced by Thermal Ceramics (Augusta, Georgia) as a filter material for automotive airbags. The paper is formed on a pilot paper machine from cylindrical alumina and silica fibers. The basis weight of these samples is 725 gsm. These samples were vacuum deaerated and soaked with water. The samples were two-sided, leading to some problems in obtaining uniform dye flow in the z-direction, especially when injecting dye into dry samples. Measurements in three vacuum-deaerated and saturated samples gave relative porosities ranging from 79% to 99%. Repeat runs with one sample gave 79% relative porosity for a 9-cm dyed zone in one run, and 83% for a 12.7-cm dyed zone in a subsequent run (the sample was resaturated for the second run). In these runs, the porosity was between 80 and 81%. In another sample compressed to a porosity of 73%, the

relative porosity value we measured was 88%. In a single run with a third sample, dye injected to 9 cm gave 88% porosity, and at 12.7 cm we calculated 99% relative porosity. The latter measurement may have been hampered by two-sidedness problems that made the visible dye region larger than the dye zone lower in the sheet. A value of 80-90% for relative porosity in these samples is about three times higher than Kyan's model would suggest.

Initially Dry Samples

We conducted a variety of tests featuring dye injection into dry blotter paper and dry ceramic paper. Such tests are of limited value, for capillary forces and chemical and physical absorption will pull water into pores that are not really open to flow. However, the "two-phase relative porosity" results will be an indication of the pore space that does not remain occupied by air bubbles after forced infiltration of water. The pore space occupied by air bubbles that could not be displaced by liquid provides some information about the pore structure.

Table 4 shows "dry relative porosity" values for three series of tests with 240-gsm blotter paper. (A subsequent measurement using blue dextran 2000 as the dye gave a relative porosity of 0.79 in a sheet at a porosity of 0.68.) These results were obtained by several operators using slightly different procedures. In spite of the scatter in the data, the amount of trapped air in the sheet appeared to be low, suggesting that there are few large voids which cannot be accessed by water as it flows and diffuses into the open structure of these papers.

Series I		Series II		Series III	
ε	Dry ε_{rel}	ε	Dry ε_{rel}	ε	Dry ε_{rel}
0.771	0.936	0.778	0.583	0.649	0.699
0.773	0.836	0.777	0.712	0.647	0.854
0.769	0.974	0.782	0.747	0.656	0.891
0.771	1.004	0.777	0.668	0.648	0.801
0.772	0.933	0.778	0.803	0.649	0.962
0.768	0.810				
AVG:	**0.916**	**AVG**	**0.703**	**AVG**	**0.841**

Table 4. Dry (apparent) relative porosity from injection into dry blotter paper sheets.

The case of water infiltration into a dry sheet involves many complications, including time-dependent swelling, surface diffusion, capillary flows, and relative permeability. However, measurements of dry relative porosity could provide useful information to assist in better understanding such flows in the future. Future work is planned using injection of nonswelling fluids to avoid water uptake into pores that would normally be unavailable to flow.

DISCUSSION

We have presented preliminary results from a study of relative porosity in paper, including a ceramic paper. Based on these results, it appears that much of the extrafiber pore space is available to flow. Adopting our results with nonswelling ceramic fibers, roughly 90% of that pore space may permit flow – at least under an in-plane pressure gradient.

Relative porosity values in paper were observed ranging from roughly 40% to over 80% in the total porosity range of 65 to 80%. These papers were not heavily refined, and based on permeability measurements in these sheets or in sheets from similar pulps, the compressed specific volume is expected to be between 1.0 cm^3/g and 1.5 cm^3/g. Fibers that

have been dried (recycled fibers or resaturated blotter paper) will have lower specific volumes than the original virgin fibers.

If we assume that 90% of the extrafiber porosity is open to flow, or $\varepsilon_{rel} = 0.9\ \varepsilon_o$, then our previous results based on specific volume can be modified to make a more realistic prediction of relative porosity. The results are shown in Figure 14. Relative porosity values for moist paper made from lightly refined pulp may typically lie between or near the curves shown.

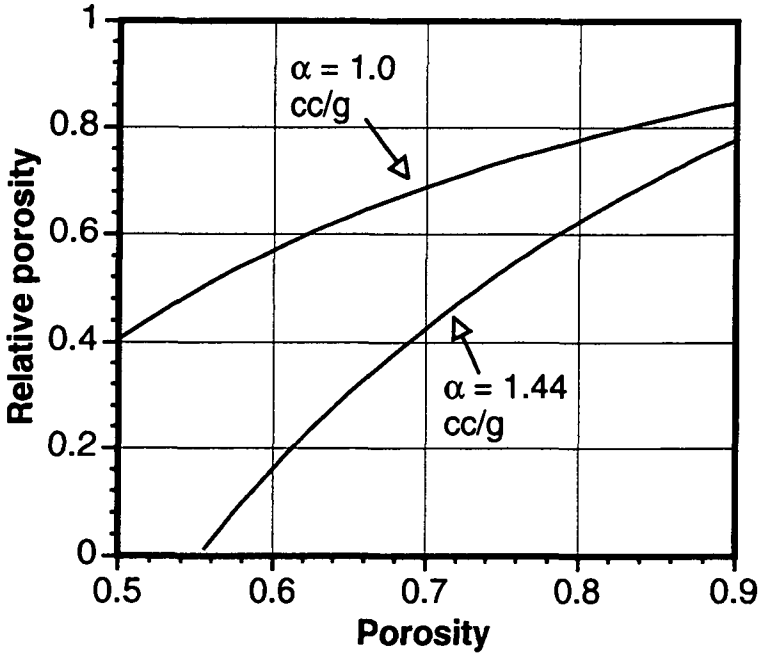

Figure 14. Predicted relative porosity results based on 90% of extrafiber pore space being open to flow. (Compare to Figure 4).

We have only considered relative porosity for in-plane flow. For flow in the transverse direction, it is possible that the differing pore structure could affect relative porosity. For example, flow normal to a flat fiber may have a stagnant zone on the downstream side of the fiber at sufficiently high particle Reynolds numbers (when inertial effects are important). In creeping flow, however, flow over a flattened fiber ought to be able to curve around the fiber surface, leaving no stagnant zones due solely to

the fiber shape. But if relative porosity is an anisotropic parameter, we would anticipate a lower value for the transverse direction than for lateral flow.

Applications

Mechanical water removal processes rely on flow of water, which must occur in the open pore space. (As compression occurs, water is squeezed from the cell walls into the open pores where it can flow; the specific volume or WRR is simultaneously reduced.) An understanding of relative porosity is relevant to the limitations of mechanical dewatering. In wet pressing, for example, as the sheet is compressed, a limit is reached when the relative porosity goes to zero in a highly compressed sheet.

Relative porosity is especially important in an alternative to wet pressing, displacement dewatering. In displacement dewatering, high densification of the sheet is avoided by using a gas phase to push liquid water out of the pores of a lightly compressed sheet. The objective is to decouple density and dryness, yielding a dewatered sheet with high bulk. This process has been investigated for several years at IPST (21). The effectiveness of the process will be directly related to the effective porosity. If the effective porosity were unity, in theory, one could hope to displace all of the liquid from the sheet (in reality, viscous fingering and capillary effects would lead to some water retention even then). In practice, we can only remove a fraction of the available water. For example, in a sheet pressed to a porosity level of 70% (giving 40% solids when saturated with water), a reasonable relative porosity value of 50% means that no more than 50% of the fluid in the compressed sheet could be displaced. If this much fluid were displaced, the solids level would be raised from 40% (for a saturated sheet) to 57% with no significant increase in densification. In practice, only about half of the water in open pores is removed by gas displacement. (This is a rough estimate.) However, the relative porosity value, if known, helps put an upper bound on what could be achieved in an ideal process.

For the penetration of ink, size, or coating color into a dry sheet, dry relative porosity tests may be of some value. Based on our tests with lateral flow, air entrapment in the pores does not seem to be a serious problem. Of course, z-direction relative porosity measurements are needed to properly address this issue.

CONCLUSIONS

The Kyan model for relative porosity appears to underpredict relative porosity values in real fibrous structures. Based on our results here, the extrafiber pore space of a paper structure is largely open to flow, with perhaps only 10% of that space truly confined to dead-end pores or stagnant zones. Of course, the details of the sheet formation will determine what fraction is open to flow. We clearly need to expand our base of results to clarify this issue.

A thorough investigation of relative porosity, or of two-phase flow processes in paper, should consider the possibility of anisotropy and velocity-dependent effects. To date, we have done neither.

Relative porosity measurements in the thickness direction of paper appear to pose serious experimental challenges. Flow rate effects will be explored, but we expect that they will be minor as long as inertial effects can be neglected (i.e., as long as Darcy's law is sufficient to describe the flow). For most papermaking operations after the forming section, inertial effects are minor (even in wet pressing).

Further work will include measurements with nonswelling fluids injected into paper to better understand the difference in pore structure between wet and dry sheets. Additional studies of recycling effects will also be carried out.

ACKNOWLEDGMENT

Thanks to Tom Merchant, Glenn Dunlap, and Ye Xiao-Liang for technical assistance in this study. This work was supported by the member companies of the Institute of Paper Science and Technology.

LITERATURE CITED

1. Roux, J. C., and Vincent, J. P., "A Proposed Model in the Analysis of Wet Pressing," Tappi J., 74(2): 189 (Feb. 1991).

2. Ellis, E. P., Jr., "Compressibility and Permeability of Never Dried Bleached Softwood Kraft Pulp and Its Application to the Prediction of Wet Press," Ph.D. Thesis, Chem. Eng. Dept., Univ. of Maine, Orono, Maine, 1981.

3. Robertson, A. A., "The Physical Properties of Wet Webs. Part 1. Fibre-Water Association and Wet Web Behaviour," Tappi J., 42(12): 969 (1959).

4. Robertson, A. A., "The Physical Properties of Wet Webs. Part 2. Fibre Properties and Wet Web Behaviour," Svensk Pappers., 66(12): 477 (1963).

5. Stone, J. E., and Scallan, A. M., "The Effect of Component Removal upon the Porous Structure of the Cell Wall of Wood. Part III. A Comparison Between the Sulphite and Kraft Processes," Pulp and Paper Canada, 69(12): 69/T288 (June 21, 1968).

6. Carlsson, G., Lindström, T., and Scöremark, C., "Expression of Water from Cellulosic Fibres Under Compressive Loading," Fibre-Water Interactions in Paper-making, Transactions of the Symposium at Oxford, Sept. 1977, British Paper and Board Ind. Fed., London, 1977.

7. Fowler, J. L., and Hertel, K. L., "Flow of a Gas Through Porous Media," J. Appl. Physics, 11: 496-502 (1940).

8. Chen, F. J., "The Permeability of Compressed Fiber Mats and the Effects of Surface Area Reduction and Fiber Geometry," Ph.D. Dissertation, The Institute of Paper Chemistry, Appleton, Wisconsin, June 1982.

9. Carroll, M., and Mason, S. G., "The Measurement of Fiber Swelling by the Liquid Permeability Method," Can. J. Tech., 30(12): 321 (1952).

10. Kyan, C. P., Wasan, D. T., and Kintner, R. C., "Flow of Single-Phase Fluids Through Fibrous Beds," Ind. Eng. Chem. Fundam., 9(4): 596 (1970).

11. Lindsay, J. D., "The Anisotropic Permeability of Paper," Tappi J., 73(5): 223 (May 1990).

12. Lindsay, J. D., and Wallin, J. R., "Characterization of In-Plane Flow in Paper," AIChE Forest Products Division Symposium Series (1992).

13. Lindsay, J. D., "The Anisotropic Permeability of Paper: Theory, Measurements, and Analytical Tools," IPC Technical Paper Series #289, The Institute of Paper Chemistry, Appleton, Wisconsin, 1988.

14. Horstmann, D. H.; Lindsay, J. D., and Stratton, R. A., "Using Edge-Flow Tests to Examine the In-Plane Anisotropic Permeability of Paper," Tappi J., 74(4): 241 (1991).

15. Adams, K. L., and Rebenfeld, L., "In-Plane Flow of Fluids in Fabrics: Structure/Flow Characterization," Textile Research J., 57(11): 647 (1987).

16. Adams, K. L.; Miller, B., and Rebenfeld, L., "Forced In-Plane Flow of an Epoxy Resin in Fibrous Networks," Polymer Eng. and Sci., 26(20): 1434 (1986).

17. Adams, K. L.; Russel, W. B., and Rebenfeld, L., "Radial Penetration of a Viscous Liquid into a Planar Anisotropic Porous Medium," Int. J. Multiphase Flow, 14(2): 203 (1988).

18. Miller, B.; Friedman, H. L., and Amundson, R., "In-plane Flow of Liquids into Fibrous Networks," 1991 Tappi Nonwovens Conference, Marco Island, Florida, May 1991.

19. Lindsay, J. D., and Brady, P. H., "Studies of Anisotropic Permeability with Applications to Water Removal in Fibrous Webs," 1992 TAPPI Nonwovens Conference, Marco Island, FL, May 1992.

20. Cussler, E. L., *Diffusion: Mass Transfer in Fluid Systems*, Cambridge Univ. Press, Cambridge, 1984, pp. 89-101.

21. Lindsay, J. D., "Displacement Dewatering to Maintain Bulk," Paperi ja Puu, 74(3): 232-242 (1992); also presented at the Helsinki Symposium on Alternate Methods of Pulp and Paper Drying, Helsinki, Finland, June 4-7, 1991.